Modeling and Optimization of the Electric Arc Furnace With Electromagnetic Stirring

Michael Lundh[1], Xiaojing Zhang[1], Jan-Erik Eriksson[2], Lidong Teng[2]

[1]ABB AB, Corporate Research
72178, Västerås, Sweden
Phone: +46 21 342862
Email: michael.lundh@se.abb.com

[2]ABB AB, Process Automation, Metallurgy Products
72159, Västerås, Sweden

Keywords: Electric Arc furnace, Modeling, Optimization

INTRODUCTION

Electric arc furnace (EAF) is an energy intensive process and one of major routes of steelmaking. EAF productivity and steel production cost are major concern for EAF technology development. ABB developed electromagnetic products for EAFs over 70 years ago. Over 150 units were installed worldwide with increased productivity, improved steel quality and operation safety. Since 2009, ABB has committed to the technology and product development of ArcSave®, a new generation of electromagnetic stirrer for EAF application. ArcSave has been investigated through numerical simulation [1], EAF water model experiments [2] and plant test with ABB previous electromagnetic stirrer [3]. ArcSave product was released in 2014 and first was installed in a 90 ton Arc furnace. Hot test results show a significant iron yield increase and other process benefits which have been presented in the AISTech 2015 conference [4].

In ABB's current efforts, advanced control and optimization for ArcSave® have been investigated in order to obtain additional process improvements through controlling scrap melting and refining processes. Non-linear first principle dynamic simulation models with electromagnetic stirring have been developed. ArcSave process simulations using - plant measurement data were performed to cover complete 3-bucket charge processes. The models were verified with liquid melt tapping temperature and carbon content measurements. In this paper, an optimal control solution is described in detail. A Modelica model of an electric arc furnace with ArcSave has been developed to formulate an optimal control problem to provide the best possible inputs during either melting or refining processes. The objectives for melting includes the arc power, the natural gas, and the remaining solid scrap. The objective for refining includes produced liquid steel, the arc power, oxygen consumption, and decarburization. Two optimization problems are studied here; scrap melting for the first bucket and also the refining processes.

DYNAMIC FIRST PRICIPLES MODEL

A non-linear dynamic model of the electric arc furnace is described in [5]. It is a modification and extension of Bekker's model [6]. Bekker's model has also been further developed in [7]. The model has eight states and eight inputs. These are described in Table 1. Outputs are not considered here since the model will only be used for simulation and optimal control. Hence, feedback from measurements will not be considered.

Table 1. Definition of states x and inputs u in the model

	States x_i		Inputs u_i
x_1	mass of solid steel [kg]	u_1	electric arc power [kW]
x_2	mass of liquid steel [kg] (including both charged carbon and carbon in scrap)	u_{2i}	oxygen injection flow [Nm3/min]
x_3	mass of dissolved carbon [kg]	u_{3i}	carbon injection flow [kg/min]
x_5	mass of solid slag [kg] (lime, dolomite, etc. as slag additions)	u_{4i}	EMS current [A]
x_6	mass of liquid slag [kg] (lime, dolomite, etc. as slag additions, not including FeO)	u_{5i}	Natural gas flow [Nm3/min]
x_7	mass of FeO in slag [kg]	u_{6i}	DRI addition flow [kg/min]
x_{12}	bath and molten slag temperature [K]	u_{7i}	Slag addition flow [kg/min] (lime, dolomite…)
x_{13}	scrap and solid slag temperature [K]	u_{8i}	Post-combustion oxygen flow [Nm3/min]

The differential equations are listed below for sake of completeness. For a full description see [5]. The model is implemented in the Modelica language [8] which is very well suited for simulation and optimization. There are a number of free and commercial software tools available for Modelica models. Some to mention are OpenModelica [9], JModelica [10], MathModelica [11], and Dymola [12]. Here MathModelica with a specific ABB extension has been used but at least OpenModelica and JModelica include similar optimization functions.

To be able to use the model for optimization a few modifications were needed. The main reason for these modification is to avoid non-physical conditions for states. Examples of such conditions are negative mass, temperature of liquid steel being lower than the melt temperature, temperature of solid steel being higher than the melt temperature. For simulation purposes it would be possible to equip the model with a number of if-statements that restricts some of the state derivatives to drive the states into non-physical regions. However, if-statements are not possible when using the model for optimization. To handle this situation, the model uses arc tangent based switching functions instead of the if-constructs. The function (1) switches from zero to one at x_0. The width of the transition interval is controlled by a, a small a makes the interval larger and not so distinct, but numerically more pleasant.

$$s(x, x_0, a) = \arctan(a \cdot (x - x_0))/\pi + 0.5 \tag{1}$$

This type of switching function will be used in the differential equations below for the model. Here $a = 0.001$ is chosen to give nice numerical properties. It is of course wise to minimize the use of the switching functions to limit the numerical complexity of the problem, so they will only be introduced where needed. The switching function (1) will be used for derivatives of x_{01}, x_{05}, x_{12} in the formulation of the optimal control problem to avoid negative masses, and liquid steel below the melt temperature.

Heat loss due to convection from hot liquids depend on the temperature difference and the mass of the solids and of the liquids, whichever is the lowest. This involves a min-function in the equations. However, the min-function, $\min(x_1; x_2)$ is not differentiable. It is approximated using the switch function (1).

$$\min(x_1, x_2) \approx g(x_1, x_2) = x_2 \cdot s(x_1, x_2, a) + x_1 \cdot s(x_2, x_1, a) \tag{2}$$

The function, g, is used both for convection for steel and for slag. The heat transfers due to convection becomes

$$\begin{aligned} p_{10}^{steel} &= k_{ther1} k_{area1} \cdot g(x_1, x_2) \cdot (x_{12} - x_{13}) \\ p_{10}^{slag} &= k_{ther5} k_{area5} \cdot g(x_5, x_6) \cdot (x_{12} - x_{13}) \\ p_{10}^{steel} &= p_{10}^{steel} + p_{10}^{slag} \end{aligned} \tag{3}$$

The mass of solid scrap is given as

$$\dot{x}_1 = -s(x_1, \varepsilon, a) \cdot \frac{M_{Fe} k_{ems}(p_{sol} + p_{10}^{steel}) x_{13}/T_{melt}}{\lambda_{Fe} + c_p(Fe_S)(T_{melt} - x_{13})} \tag{4}$$

where p_{sol} is arc power affecting the solid steel and where k_{ems} is a function of the stirring effect from EMS operating current.

It is described by

$$k_{ems} = a_i \sqrt{u_4} + 1 \tag{5}$$

where a_i is EMS effect parameter. When EMS is switched off, the EMS specific effect, $k_{ems}=1$.

The mass of the liquid steel is affected by melting, by iron oxidation to FeO through oxygen injections, and by recovery of FeO to Fe by carbon injections and by dissolved carbon.

$$\dot{x}_2 = s(x_1, \varepsilon, a) \cdot \frac{M_{Fe}\, k_{ems}\, (p_{sol} + p_{10}^{steel})\, x_{13}/T_{melt}}{\lambda_{Fe} + c_p(Fe_S)(T_{melt} - x_{13})}$$
$$- \frac{2M_{Fe}}{M_{O_2}} u_2 + k_{dC\_ems}\, k_{dC}\, \frac{M_{Fe}}{M_C}(X_C - X_C^{eq}) + \frac{x_7 k_{gr} M_{Fe}}{(x_6 + x_7)M_C} u_3 + 0.93 u_6 \tag{6}$$

The last term refers to DRI addition where it is assumed that DRI contains about 93% Fe [6]. Further we use $\varepsilon = 100$ here. The switching function will set the melt rate to zero when there is no more material to melt.

The mass of dissolved carbon is determined by the decarburization reaction rate. Since EMS has a positive effect on the decarburization reaction, the rate is proportional to EMS stirring power. The decarburization rate can be described by

$$\dot{x}_3 = - k_{dC}\, k_{dC\_ems}\, (X_C - X_C^{eq}) \tag{7}$$

$$X_C = \frac{x_3/M_C}{x_2/M_{Fc} + x_3/M_C} \tag{8}$$

$$X_C^{eq} = k_{XC}\, k_{dC\_ems} \left(\frac{x_6 M_{FeO}}{x_7 M_{slag}} + 1 \right) \tag{9}$$

The equations for mass of the solid slag and of the liquid slag are given by

$$\dot{x}_5 = -s(x_5, \varepsilon, a) \cdot \frac{M_{slag}\, k_{ems}\, p_{10}^{slag} \cdot x_{13}/T_{melt}}{\lambda_{slag} + c_p(slag_S)(T_{melt} - x_{13})} + u_7 \tag{10}$$

$$\dot{x}_6 = s(x_5, \varepsilon, a) \cdot \frac{M_{slag}\, k_{ems}\, p_{10}^{slag} \cdot x_{13}/T_{melt}}{\lambda_{slag} + c_p(slag_S)(T_{melt} - x_{13})} \tag{11}$$

Here $\varepsilon = 10$ in the optimization.

The mass of FeO in the slag is given by

$$\dot{x}_7 = \frac{2M_{FeO}}{M_{O_2}} k_{ems\_o2}\, u_2 - \frac{x_7 k_{gr} M_{FeO}}{(x_6 + x_7)M_C} u_3 - \frac{M_{FeO}}{M_C} k_{dC}\, k_{dC\_ems}\, (X_C - X_C^{eq}). \tag{12}$$

Depending on the initial conditions, x_7 may need to be restricted to be non-negative. However, this has not been found necessary with the initial conditions that have been used.

The temperature of the liquid steel and slag must not be below the melt temperature. The power used for increasing the liquid temperature is a sum of power distributed to the liquid, chemical reaction power and various heat losses. The liquid temperature can be calculated as.

$$\dot{x}_{12} = s(x_{12}, T_{melt}, a) \cdot \frac{p_{liq} + p_{ch} - p_{cool-wt} - p_6 - p_8 - p_9 - p_{10}}{\dfrac{C_p(Fe_L)}{M_{Fe}} x_2 + \dfrac{C_p(C)}{M_C} x_3 + \dfrac{C_p(Si)}{M_{Si}} x_4 + \dfrac{2x_6 + 2x_7}{M_{slag}} C_p(slag)} \tag{13}$$

where x_4 is the mass of silicon in the liquid steel and it is treated as a parameter instead of a state. The model captures also power losses to cooling water $p_{cool-wt}$ and to leak air p_6. These are assumed to be constant in the simulations. Power used to heat-up solid scrap, lime, dolomite, DRI, and extra carbon charge to the melting points is also accounted for, p_7, p_8, and p_9.

The scrap and solid slag temperature is given by

$$\dot{x}_{13} = \frac{(p_{sol} + p_{10})\,(1 - \frac{x_{13}}{T_{melt}})}{\frac{c_p(Fe_S)}{M_{Fe}} x_1 + \frac{2c_p(slag_s)}{M_{slag}} x_5}$$

(14)

The temperature of the solid steel and slag must not exceed the melt temperature. A limitation is provided for this in the optimization.

The values of the parameters in the model have been determined to adapt the model behavior to logged data. These parameters have been used throughout optimizations presented here. Their values are found in the Appendix.

OPTIMIZATION

The above model was implemented in Modelica using MathModelica. The specific ABB extension was used to convert the model to an optimization problem to solve an optimal control problem. The solution is the optimal trajectories for the inputs that takes the electric arc furnace from a given initial state to a final state while minimizing a loss function and satisfying given constraints. This loss function could be to minimize the time for the state transition. The resulting optimization problem is solved using IPopt [13].
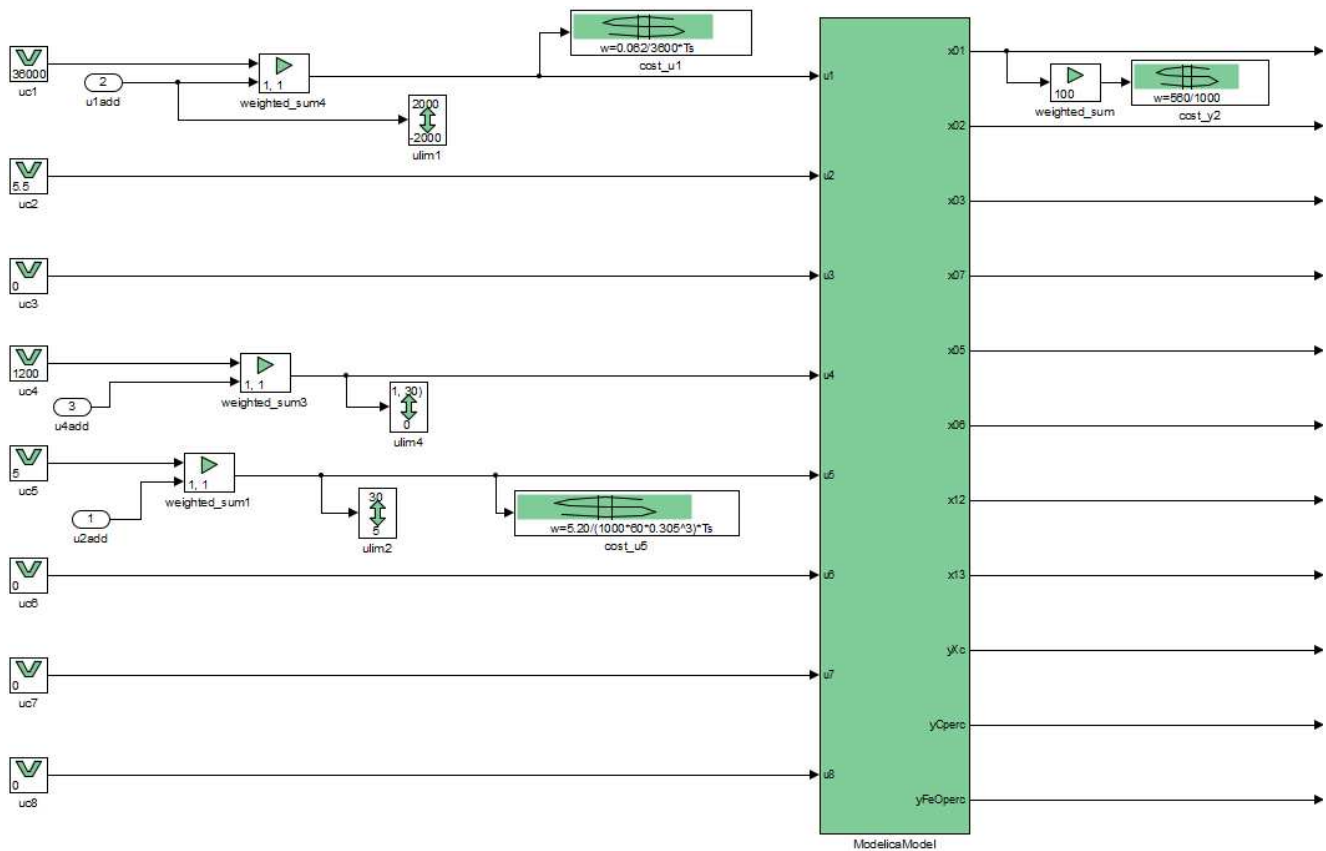
Figure 1 Model for melting optimization

Melting

The first example handles the melting of steel in the first basket. Figure 1 shows the model for melting optimization. The main block is the Modelica model which was exported from MathModelica. Eight inputs are defined to the model. These are either a nominal trajectory or the sum of a free variable and a nominal trajectory. The nominal trajectories were obtained from a simulation with nominal (constant) inputs to the model. The starting values at the collocation points for the optimization were obtained through interpolation in the simulation result. By this approach u=0 should be a feasible solution

to the optimal control problem since it describes the deviation from the nominal trajectory. The optimization problem becomes easier to solve then. Table 2 shows the initial states for the optimization of the melting of the first basket. Three inputs are free in the optimization here, u_1, u_4, and u_5.

Table 2 Initial states for melting optimization

State	Initial Value	Unit	Description
x01	49745	kg	Solid steel
x02	15000	kg	Liquid steel
x03	670	kg	Dissolved carbon
x05	1578	kg	Solid slag
x06	1000	kg	Liquid slag
x07	2.3	kg	FeO in liquid slag
x12	1800	K	Bath and molten slag temperature
x13	300	K	Scrap and solid slag temperature

The objective is to minimize sum of three components:

- Cost of electric arc power, c_{el}.

- Cost for added natural gas for burners, c_{ng}.

- Cost of remaining solid scrap, c_{sc}. This is an artificial cost to force the steel melting.

Mathematically we have

$$c_{el} = \frac{0.0620}{3600} \cdot \int_0^T u_1 \, dt \tag{15}$$

$$c_{ng} = \frac{4.20}{1000 \cdot 60 \cdot 0.305^3} \cdot \int_0^T u_2 \, dt \tag{16}$$

$$c_{sc} = 10 \frac{560}{1000} \cdot \int_0^T x_1 \, dt \tag{17}$$

where T is the end time. The integrals and the variables in the model are discretized over 100 collocation points were evenly spread over a 1400 s long interval. The constants before the integrals reflect the price.

The loss function penalizes the amount of solid scrap. Hence, this loss function will drive the solid scrap to zero as fast as possible. Figure 2 shows the trajectories for the inputs and Figure 3 shows trajectories for the solid scrap (x_1). Each figure shows two trajectories; solid lines show the optimal trajectory and dashed lines shows the simulation with nominal inputs.

In the melting phase it seems beneficial to use all available power, i.e. maximize the arc power (u_1) and the natural gas flow (u_5). The electromagnetic stirrer (u_4) will also use as high current as it is allowed to. In the beginning it is constrained to be switched off for the first 420 s, since there is not enough liquid steel. There is not much difference between the initial and the optimal trajectory. Melting time is affected by the added power. For fastest melting, use all available power.
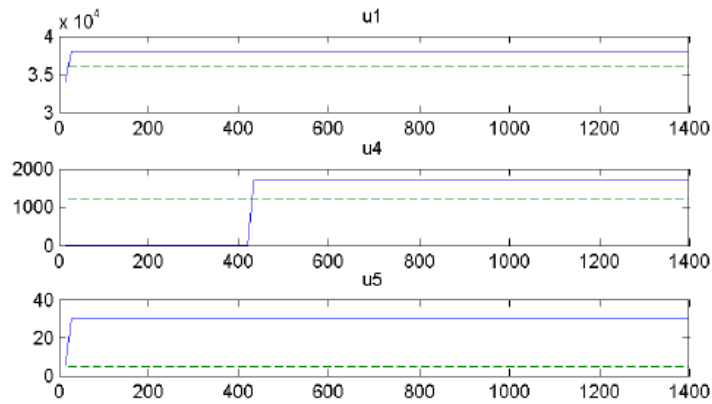
Figure 2 Input trajectories for optimal melting (solid) and for nominal melting (dashed).
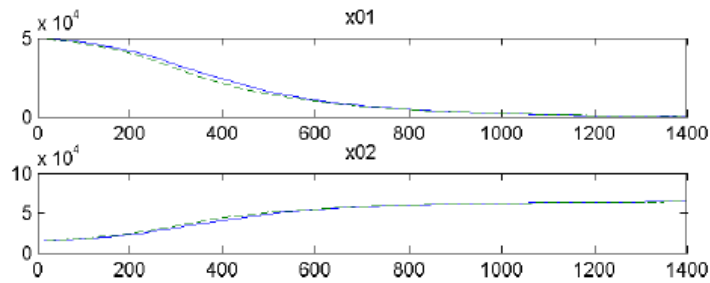
Figure 3 Optimal melting trajectory (solid) and nominal melting (dashed).

Refining

This example handles the refining of steel after the third basket has been loaded. Table 3 shows the initial states for the optimization of the refining. Four inputs are free in the optimization here, u_1, u_2, u_3, and u_4. The refining phase is completed when the liquid steel has reached the desired temperature and the carbon content of the steel reaches a certain value. To reach this in an optimal way an optimization problem is defined using an objective function and some constraints. The objective function minimizes a sum of four components:

- Cost of electric arc power, c_{el}.

- Cost for added oxygen, c_{o2}.

- Cost for added carbon, c_c.

- Negative value of produced liquid steel, c_{st}. This component is the profit, and therefore has negative sign in the cost function.

Table 3 Initial states for optimization

State	Initial Value	Unit	Description
x01	7860	kg	Solid steel
x02	107000	kg	Liquid steel
x03	250	kg	Dissolved carbon
x05	920	kg	Solid slag
x06	3240	kg	Liquid slag
x07	273	kg	FeO in liquid slag
x12	1809	K	Bath and molten slag temperature
x13	1218	K	Scrap and solid slag temperature

The discretized loss function which will be minimized in the optimal control problem becomes

$$J = \sum_{t=T_s}^{100T_s} \left(\frac{0.0620}{3600} \cdot u_1(t) + \frac{4.20}{1000 \cdot 60 \cdot 0.305^3} \cdot u_2(t) + \frac{250}{1000 \cdot 60} \cdot u_3(t) \right) \cdot T_s - \frac{560}{1000} \cdot x_2(100T_s) + (sc) \tag{18}$$

where T_s is the time discretization step and (sc) are additional penalties to the loss function to satisfy soft constraints in the optimization. The following soft constraints were defined:

- The final temperature for liquid steel, x_{12}, should stay between 1940 K and 1960 K.

- The final carbon content of the steel should be below 0.1%.

There is no requirement of FeO content since a high value here would lead to decreased yield which would lead to a smaller final x_2 and a higher value of the objective function. The cost functions and soft constraints can be seen in Figure 4, where also some hard constraints on the inputs are defined. Here, 100 collocation points were evenly spread over an 1100 s long interval. Figure 5 shows the trajectories for the inputs (left) and the trajectories for some of the states (right).

An optimal control law will in many cases lead to control signals that switch between their extreme values during the period for the optimization. This is also the case here. The optimization maximizes the oxygen flow (u_2) and minimizes the graphite flow (u_3) up to the time when the liquid steel has reached the desired temperature. For some reason, yet to be investigated, the electromagnetic stirring is turned off for a short period. The behavior of these inputs is somewhat different compared to what is seen during a normal refining phase for this EAF where the desired tapping temperature is reached in about 1400 s. With the optimal inputs, obtained here, the tapping temperature is reached in less than 1100s. The resulting mass of liquid steel, x_2, will be higher and the final FeO content will be kept low. The oxygen addition is stopped after a certain interval, which also could be seen as a reduction of the total amount of added oxygen. A cautions assessment of the oxygen reduction could be estimated through the following way: Figure 5 shows that the added oxygen is constant throughout the refining period. If we here compare the 1100 s long refining period with full oxygen addition with the optimal oxygen addition, which is turned off after 900 s, then the oxygen reduction is 200/1100 (about 18%).

Figure 6 shows a close up of the carbon percentage in the steel and the FeO percentage in the liquid slag. Here we see that the optimal solution decreases the final FeO content, while the final carbon content is affected very little.
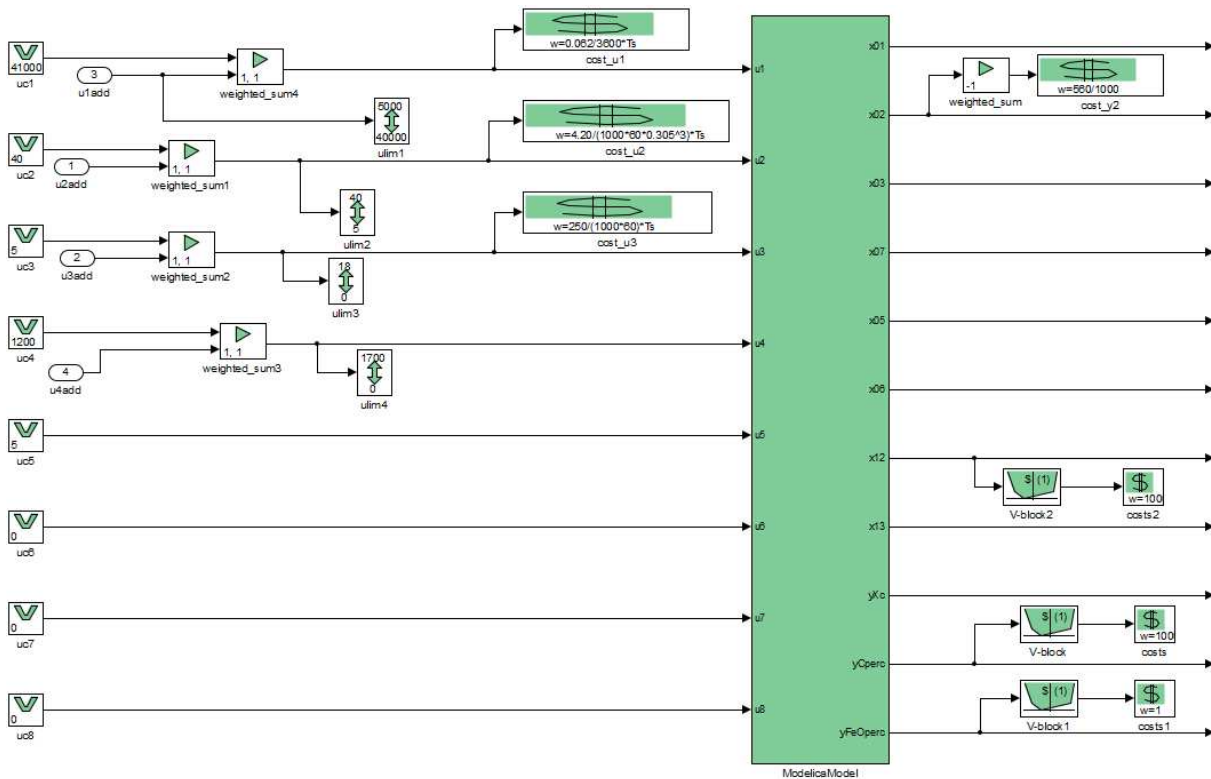
Figure 4 Model for refining optimization
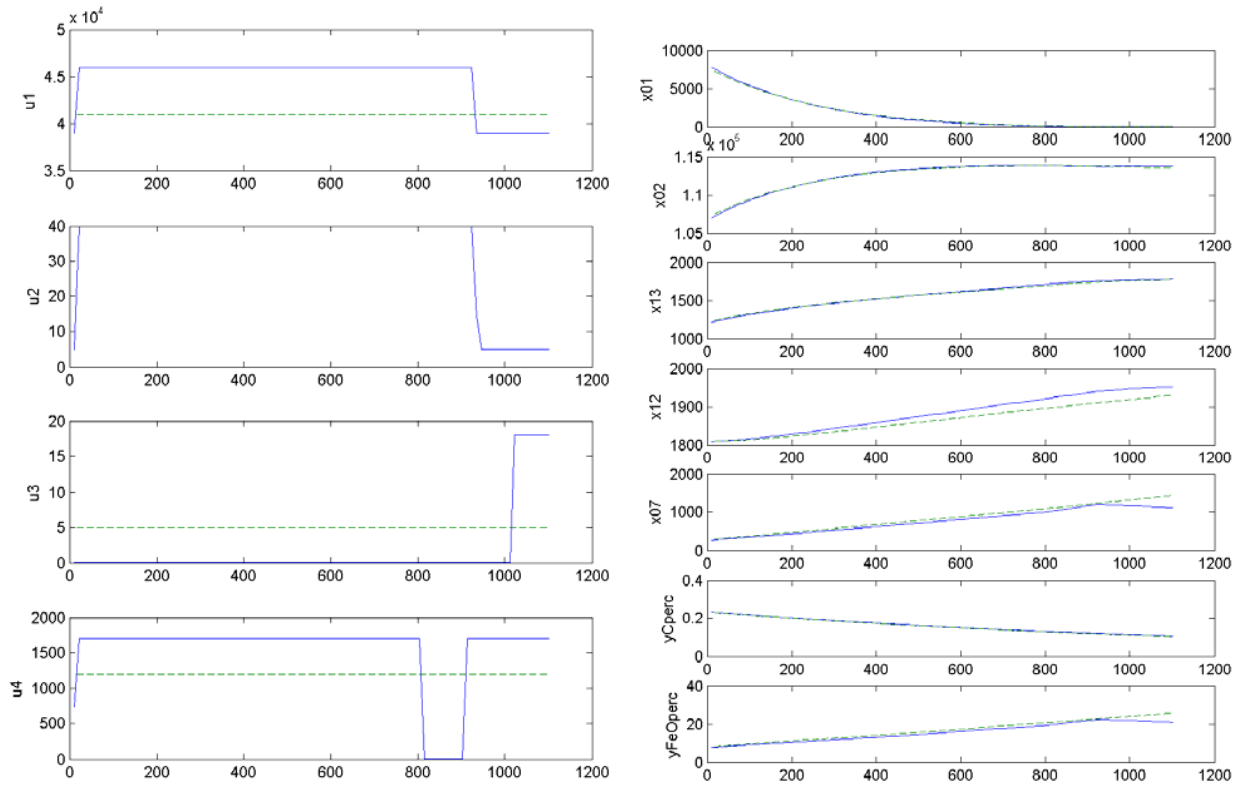
Figure 5 Input (left) and output (right) trajectories for optimal refining

The drop in stirring current for optimal refining in Figure 5 is somewhat difficult to explain. Also it would be interesting to see how much the arc power would decrease at the end, if the lower bound of it was decreased. To investigate the impact of this, four additional optimizations were done with slightly modified bounds on the inputs. The result is shown in Table 4. The first row corresponds to the bounds used in Figure 5, and the second row corresponds to a case where the stirring current is forced to be almost at it maximal value. The difference in final values is small.

Rows three and four in Table 4 show similar cases, but here also the arc power is allowed to become zero. This causes the value of the objective function to decrease with about 7% since the arc power becomes low in the end of the optimization. The arc power does not become zero, but rather takes values about 18000 kW in the end. This is seen in Figure 7. It is also worth to mention that no carbon was added in the optimizations corresponding to rows three and four.

Table 4 Final values for different limits on arc power and stirring current.

u_1	u_4	x_{01}	x_{02}	x_{13}	x_{12}	x_{07}	%C	%FeO	J
39-46	0-1700	51	113792	1790	1952	1108	0.105	21.0	6.26e6
39-46	1690-1700	50	113781	1790	1953	1065	0.105	20.4	6.28e6
0-46	1690-1700	51	113744	1789	1940	1106	0.104	21.0	5.89e6
0-46	0-1700	52	113757	1789	1940	1148	0.105	21.6	5.88e6
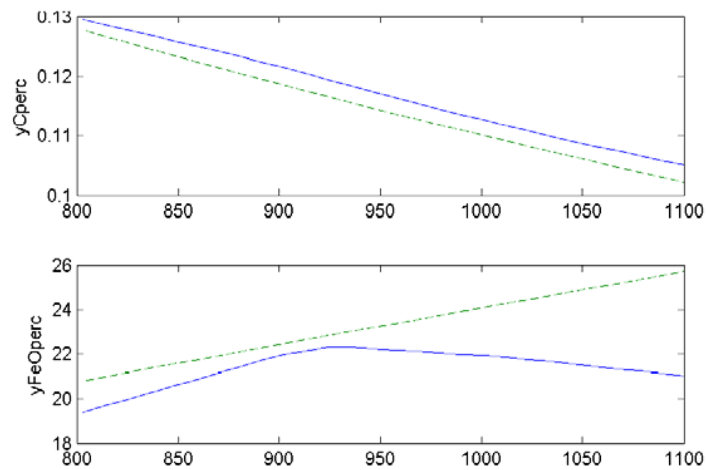
Figure 6 Optimal refining trajectory
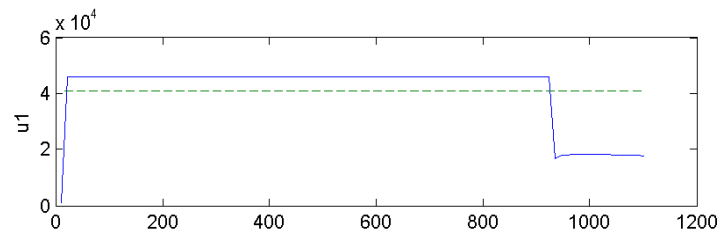
Figure 7 Input trajectory for arc power for optimal refining for zero low limit on arc power

CONCLUDING DISCUSSION

A Modelica simulation model has been developed to simulate complete EAF scrap melting and refining processes with 3-bucket charge, and to optimize EAF operation to reach optimal total cost saving of electric arc power, natural gas, oxygen and added carbon. The model is validated using plant measurement data and it has been used to evaluate the effect of stirring during melting and refining. The optimal control problems were solved to suggest optimal trajectories for the inputs to EAF during melting and refining. The results showed that the approach for finding the optimal input trajectories for EAF is valuable to understand what could be achieved, and how the ideal control of the electric arc furnace would be. The stirring power obtained from the optimal control problems indicates that it is beneficial to stir as much as possible. In the practical operation, a dynamic stirring profile has to be optimized based on the individual arc furnace process.

REFERENCES

1   O. Widlund, U. Sand, O. Hjortstam, and X. Zhang, "Modeling of Electric Arc Furnaces (EAF) with Electromagnetic Stirring", Proc. of 4th Int. Conf. on Modelling and Simulation of Metallurgical Processes in Steelmaking (SteelSim), Metec InSteelCon 2011, Stahlinstitut VDEh, Düsseldorf, Germany, 2011

2   M. A. Rahmani, X. Zhang, O. Widlund, H. Yang, and J.E. Eriksson, C. Carlsson, ''A Water Model Study of Vortex Formation and Prevention during Tapping of an EBT-type EAF'', In: 8th International Conference on Clean Steel, 14 –16 May 2012, Budapest, Hungary

3   X. Zhang, H. Yang, O. Widlund, J.E. Eriksson, and E. Rahkola, "Analysis of the Process Improvement in Electric Arc Furnaces by Electromagnetic Stirring", In: 8th International Conference on Clean Steel, 14 –16 May 2012, Budapest, Hungary

4   L. Teng, A. Jones, H. Hackl, M. Meador, "ArcSave®, Innovation Solution for Higher Productivity and Lower Cost in the EAF", AISTech 2015 proceedings, 2015.

5   X. Zhang, M. Lundh, L. Teng, J-E. Eriksson and C-F. Lindberg, "Process Modeling and Simulation of EAF with electromagnetic stirring", MS&T14, 12-16 October 2014, Pittsburgh, USA

6   J.G. Bekker, I.K. Craig, and P.C. Pistorius, "Modeling and Simulation of an Electric Arc Furnace Process", ISIJ International, 39(1):23–32, 1999

7   V. Logar, D. Dovzan, and I. Skrjanc, "Modeling and Validation of an Electric Arc Furnace: Part 1, Heat and Mass Transfer", ISIJ International, 52(3):402–412, 2012

8   Modelica, Modelica Association, www.modelica.org

9   OpenModelica, www.openmodelica.org

10   JModelica, www.jmodelica.org

11   MathModelica System Designer, User Guide. MathCore Engineering AB, Linköping, Sweden, 2007. (Now provided by Wolfram), www.wolfram.com/system-modeler

12   CATIA Systems Engineering – Dymola, www.3ds.com/products-services/catia/products/dymola

13   A. Wächter. Introduction to IPopt: A tutorial for downloading, installing, and using IPopt, 2008

APPENDIX

Model parameters are defined in the table below. These relate to a specific electrical arc furnace.

Parameter	Value/Unit	Description
a_1	-	EMS gain factor for melting
kdC	12	Bath decarburization rate
$kdCeq\_ems$	1	EMS effect on $Xceq$
kgr	0.76	Graphite injection effect of FeO in slag
$kpostliq$	0.2	Factor for post-combustion effect on liquid steel
$kther1$	0.4 kW/K m2	Heat transfer coefficient
$kther5$	0.2 kW/K m2	Solid slag melting rate
$ku1$	0.2	Factor for arc effect on liquid steel
$ku5$	0.5	Factor for arc effect on liquid steel
$ku5liq$	0.2	Factor for burner effect on liquid steel
$kwater$	12	Heat transfer coefficient
kXC	0.000491	Equilibrium concentration constant
$Tair$	298 K	Air temperature
$TDRI$	293.15 K	DRI temperature
$Tmelt$	1800 K	Scrap melting temperature
x_{14}	7 Pa	Absolute pressure
$x_{4\ av}$	118 kg	Silicon in solution in steel
x_8	600 kg	Silicon dioxide in slag